Infrared Spectroscopy of the Topological Surface States of Bi_2Se_3 by Use of the Berreman Effect

Enrico Falsetti,[1] Alessandro Nucara,[1] Pavel P. Shibayev,[2] Maryam Salehi,[3] Jisoo Moon,[2] Seongshik Oh,[2] Jean-Blaise Brubach,[4] Pascale Roy,[4] Michele Ortolani,[1] and Paolo Calvani[1]

[1]*Dipartimento di Fisica, Università di Roma La Sapienza, Piazzale Aldo Moro 2, I-00185 Roma, Italy*

[2]*Department of Physics and Astronomy, Rutgers, the State University of New Jersey, Piscataway, New Jersey 08854, USA*

[3]*Department of Materials Science and Engineering, Rutgers, the State University of New Jersey, Piscataway, New Jersey 08854, USA*

[4]*Synchrotron SOLEIL, L'Orme des Merisiers Saint-Aubin, BP 48, F-91192 Gif-sur-Yvette Cedex, France*

(Received 11 August 2018; published 24 October 2018)

The Berreman effect (BE) allows one to study the electrodynamics of ultrathin conducting films at the surface of dielectrics by use of grazing-angle infrared spectroscopy and polarized radiation. Here, we first apply the BE to the two-dimensional electron system (2DES) at the interface between a high-purity film of the topological insulator Bi_2Se_3 and its sapphire substrate. We determine for the 2DES a charge density $n_s = (8 \pm 1) \times 10^{12}$ cm^{-2}, a thickness $d = 0.6 \pm 0.2$ nm, and a mobility $\mu^{IR} = 290 \pm 30$ cm^2/V s. Within errors, all of these parameters result in being independent of temperature between 300 and 10 K. These findings consistently indicate that the 2DES is formed by topological surface states, whose infrared response is then directly observed here.

DOI: 10.1103/PhysRevLett.121.176803

An ideally pure Bi_2Se_3 single crystal or thin film is a three-dimensional topological insulator (TI) where a two-dimensional electron system (2DES) forms spontaneously at the interface with another dielectric due to the peculiar topology of the TI electronic bands, which are dominated by strong spin-orbit effects [1–3]. The topological surface states (TSSs) in the 2DES are protected from backscattering by a strong coupling between spin and momentum, so their mobility is remarkably high and virtually constant up to room temperature [4]. However, in real samples, a finite amount of Se vacancies are always present. They provide free electrons at virtually all temperatures due to the high permittivity (∼110) and low effective mass ($m^* \simeq 0.20 m_e$) characteristic of Bi_2Se_3 [5]. In order to match the bulk chemical potential with the Fermi energy [6] of the TSSs, a band bending occurs at the TI surface, which may attract or repel part of those carriers. In the frequent occurrence of downward band bending, a charge-transfer (CT) process accumulates electrons from the bulk to the surface. Their density n_{CT} thus may add to the TSS density n_{TSS}, possibly obscuring the topological contribution to the surface electrodynamics. The thickness d of the surface carrier layer at the Bi_2Se_3 surface has been estimated to be between 3 and 1 nm [6–8], of the same order of magnitude as that which forms at the interface between $LaAlO_3$ (LAO) and $SrTiO_3$ (STO) [9,10], and then can be considered as a 2DES. Recently, thin films of Bi_2Se_3 deposited by molecular beam epitaxy (MBE) on sapphire (Al_2O_3) substrates have displayed total charge densities very similar to those expected for a 2DES formed by TSSs alone [6], demonstrating the high purity of the film. This result has allowed for a direct inspection of the 2DES in thin Bi_2Se_3 films by several experimental tools, including infrared spectroscopy (IRS). For example, IRS has been successfully used to detect the 2DES plasmonic excitations in lithographically patterned Bi_2Se_3 films [11,12].

In Bi_2Se_3 thin films, one 2DES forms at the film-vacuum interface, and another one at the film-substrate interface. Here, we use IRS to study the electrodynamics of the 2DES at the TI-sapphire interface, by exploiting the Berreman effect (BE) [13]. This technique allows one to detect the longitudinal excitations of ultrathin polar systems, such as vibrations of adsorbed layers or the Drude absorption of 2D free-electron systems. For instance, it has been successfully employed to measure in a noncontact mode the conducting properties of the quasi 2DES at the $LaAlO_3/SrTiO_3$ interface [10,14,15], a few nanometers thick. The BE exploits the strong electric dipole that the component of the radiation electric field in the plane of incidence (p component) creates when entering a film of thickness d much smaller than both the radiation wavelength λ and the field penetration depth d_p. For a conducting layer at the interface between two dielectrics, as in $LaAlO_3/SrTiO_3$ or here in Bi_2Se_3/Al_2O_3, a BE resonance is expected to appear at a radiation frequency ω such that the real part $\epsilon_1(\omega)$ of the dielectric function $\tilde{\epsilon}(\omega)$ of either dielectric is zero. As the only strong optical phonon of Bi_2Se_3 (α mode) falls in the terahertz range [16], one here may look for the BE at the strong and narrow LO phonons of the substrate, similar to what is done for detecting the BE at the interface

$LaAlO_3/SrTiO_3$ [10,14,15] with a strong phonon of $SrTiO_3$. One may notice that the observation of the BE due to the 2DES is insensitive to the fact that the longitudinal optical phonon oscillation takes place in the material hosting the interfacial 2DES (STO in the case of the LAO/STO interface) or in the substrate in close contact with the 2DES (sapphire in the present case).

The BE resonance is a very weak feature. Indeed, once the above conditions $d \ll \lambda$, $d \ll d_p$ are satisfied, its intensity decreases rapidly for $d \to 0$. The optimum thickness for the observation of an ultrathin layer by the Berreman effect is [17]

$$d_{\mathrm{opt}} = (\lambda/2\pi)(\cos\theta/\sin^2\theta)\Xi_{\mathrm{max}}, \tag{1}$$

where θ is the angle of incidence and Ξ_{max} is the value at resonance of the energy loss function $\Xi = \mathrm{Im}[-1/\tilde{\epsilon}]$. For example, in the quasi 2DES at a LAO/STO interface, d_{opt} is approximately [10] 50 nm, a value much larger than its actual thickness of a few nanometers. Even if our optics with a single polarizer do not implement an ellipsometric setup, it is useful to express the results in terms of the ellipsometric angle

$$\Psi(\omega) = \arctan[(R_p/R_s)^{1/2}], \tag{2}$$

where R_p (R_s) is the sample reflectivity in p (s) polarization. If moreover $\Psi_{\mathrm{film+sub}}(\omega)$ is the angle measured on the TI-sapphire system and $\Psi_{\mathrm{sub}}(\omega)$ is that of the bare sapphire substrate, separately measured, their difference

$$\Delta\Psi(\omega) = \Psi_{\mathrm{film+sub}}(\omega) - \Psi_{\mathrm{sub}}(\omega) \tag{3}$$

will show the typical Berreman feature made of a narrow dip followed by a broad peak at higher frequency, induced by the presence of the 2DES at the TI-sapphire interface. Indeed, the opposite 2DES at the TI-vacuum interface cannot contribute to the present observations because its direct absorption—in the absence of BE—is vanishingly small in our frequency range. One can also exclude any electromagnetic interaction between the TSSs at the two interfaces, as their distance (120 nm) is much larger than the range of such an interaction [18]. By using Eq. (3) and polarized radiation at grazing incidence, we detected Berreman resonances at the reflectivity edges of two LO phonons of sapphire, at 391 and 482 cm^{-1} (at 300 K). Then, by using Fresnel formulas for the optical response of a multilayer [10,19], and Drude-Lorentz fits, we extracted from the spectra the parameters of the 2DES. We could thus collect strong indications that the observed conducting layer is indeed formed by topological surface states.

High-quality Bi_2Se_3 thin films, 120 nm thick, were prepared by molecular beam epitaxy using the standard two-step growth method developed at Rutgers University [8,20]. The $10 \times 10\ \mathrm{mm}^2$ Al_2O_3 substrates were first cleaned by heating to 750 °C in an oxygen environment to remove organic surface contamination. The substrates were then cooled to 170 °C, and an initial set of three quintuple layers of Bi_2Se_3 was deposited. This was followed by heating to 300 °C, at which the remainder of the film was deposited to achieve the target thickness. The Se:Bi flux ratio was kept to 10:1 to minimize Se vacancies.

The reflectances R_p and R_s (in p and s polarization, respectively) of the bare sapphire substrate and of the TI-sapphire system were measured under an angle of incidence $\theta = 72°$, by combining a Bruker IFS125 HR interferometer with the infrared synchrotron radiation source of the AILES beam line at the SOLEIL storage ring [21,22]. The interferometer was equipped with a 6 μm beam splitter and with a bolometer from IR Labs. The spectra resulted from averaging 300 scans recorded at 80 kHz with 2 cm^{-1} resolution. The samples were thermoregulated within ± 1 K by means of a closed-cycle He cryostat from CryoMec. A gold mirror placed at the same position as the sample, and aligned parallel to it by a laser beam, was used as reference. A single polyethylene polarizer that could be remotely rotated was placed on the radiation path. The optics of the interferometer limited the energy of the incident radiation below 1000 cm^{-1}, a value lower than the band gap of Bi_2Se_3 [16], thus preventing its possible photodoping. The reflectances R_p and R_s thus obtained on the Bi_2Se_3 film deposited on Al_2O_3, and on the bare sapphire substrate, are shown in Figs. 1(a) and 1(b), respectively. The spectra in Fig. 1(b) are fully consistent with the reflectivity of sapphire at high angle of incidence reported in the literature [23,24].

The solid lines in Fig. 2 show the ellipsometric angle Ψ from Eq. (2) at three temperatures, in the region of the LO1 and LO2 longitudinal phonons of sapphire peaked (at 300 K) at 391 and 482 cm^{-1}, respectively, as obtained from Eq. (2) applied to the spectra in Fig. 1. Thanks to the excellent signal-to-noise ratio achieved by infrared SR, we could detect the reproducible differences $\Delta\Psi(\omega) = \Psi_{\mathrm{film+sub}}(\omega) - \Psi_{\mathrm{sub}}(\omega)$ plotted in Fig. 3. Therein, $\Delta\Psi(\omega)$ shows at all temperatures the expected Berreman resonance formed by a dip followed by a broad peak at higher frequency. The fluctuations with temperature of the dip broadening have no physical meaning [25], while the dip depth is related to the plasma frequency of the conducting layer [10], and then to the 2DES charge density N. The peak also provides a measurement of the carrier relaxation rate Γ_D. As one can see, the dip amplitude (and then N) is basically independent of T, as expected for a metallic system. The curves in Fig. 3 were fit to the usual Fresnel equations [10,19], which relate the reflectivity of a multilayer optical system, in both polarizations, to the dielectric function of the individual layers. Here, the fit was applied to the present three-layer system made of (i) a vacuum, which includes the bulk of the Bi_2Se_3 film which is

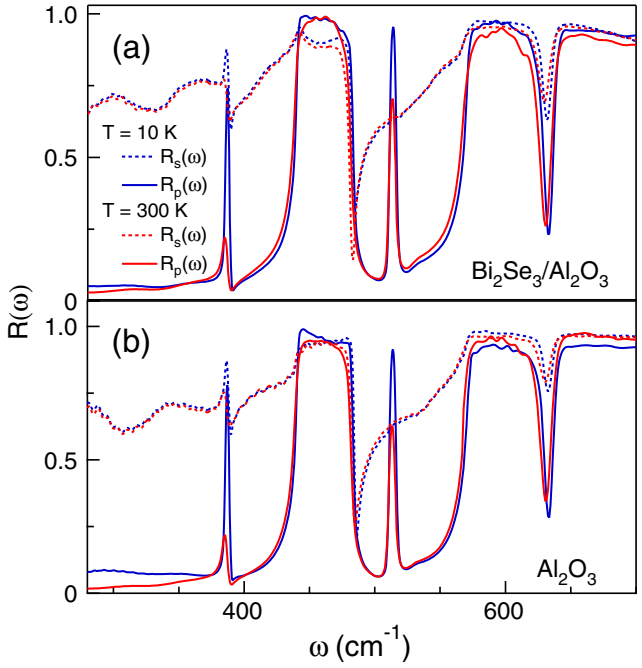

FIG. 1. Reflectivity in p and s polarization, at two temperatures, (a) of a Bi_2Se_3 film on Al_2O_3 and (b) of a bare Al_2O_3 substrate.

transparent in the present frequency range, (ii) a conducting ultrathin layer of Bi_2Se_3 having thickness d, plasma frequency ω_p, and relaxation rate Γ_D, and (iii) a semi-infinite Al_2O_3 insulating substrate whose phonon spectrum is modeled by the Lyddane-Sachs-Teller dielectric function [26],

$$\tilde{\epsilon_2}(\omega) = \epsilon_\infty \prod_j \frac{(\Omega_{Lj}^2) - \omega^2 + i(\Gamma_{Lj})\omega}{(\Omega_{Tj}^2) - \omega^2 + i(\Gamma_{Tj})\omega}. \quad (4)$$

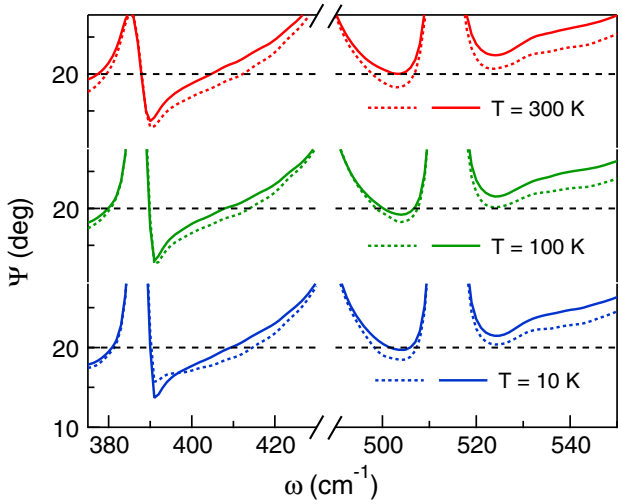

FIG. 2. Ellipsometric angles Ψ at three temperatures, from Eq. (2) and the data in Fig. 1, in the region of the (a) LO1 and (b) LO2 phonons of sapphire. Solid lines refer to the TI-sapphire system, dotted lines to the bare sapphire substrate.

Therein, ϵ_∞ is the contribution to the dielectric function from oscillators at energies higher than the phonon energies and Ω_{Lj} and Ω_{Tj} are the central frequencies of the longitudinal and transverse optical phonons, respectively, while Γ_{Lj} and Γ_{Tj} are the corresponding linewidths.

Details of the fitting procedure and an explanation of the assumptions we made are given in the Supplemental Material (SM) [27]. In Fig. 3, the fitting curves obtained by the above procedure are reported with solid lines. The resulting parameters of the Drude model for the conducting film are listed in Table I, together with those of the sapphire phonons LO1 and LO2 which trigger the resonance. As one may notice in the table, all of the fitting parameters of the conducting layer are scattered vs temperature within a small interval that can be reasonably ascribed to the propagation of the experimental error. One can then average out their values at the three temperatures and at resonances both 1 and 2, assuming that spread as the final error on the parameters. We thus obtain at any T, $d = 0.6 \pm 0.2$ nm, $\omega_p = 8050 \pm 400$ cm^{-1}, and $\Gamma_D = 220 \pm 30$ cm^{-1}. By using the Drude formula for the plasma frequency $\omega_p = [(Ne^2)/(\epsilon_0 m^* m_e)]^{1/2}$ (in rad/s), where N is the bulk charge density, $m^* \simeq 0.20$ is the carrier effective mass [28], and m_e is the electron mass, one finds $N = (1.3 \pm 0.1) \times 10^{20}$ cm^{-3}. This leads to a surface charge density $n_s = (8 \pm 2) \times 10^{12}$ cm^{-2} and, from the above value of Γ_D, to a carrier mobility $\mu^{\mathrm{IR}} = 290 \pm 30$ cm^2/V s. The former value is in very good agreement with the independent determination of $n_s \sim 1.9 \times 10^{13}$ cm^{-2}, measured in Ref. [28] in the terahertz range, for the total charge density on both Bi_2Se_3 surfaces. This reduces to $n_s \sim 9 \times 10^{12}$ cm^{-2} for the TI-sapphire interface only, observed here, by assuming in a first approximation that the two charge densities are the same. The present value of the mobility, in turn, can be compared with the previous dc estimates $\mu^{\mathrm{dc}} = 400$ cm^2/V s of Ref. [8], or μ^{dc} from 350 to

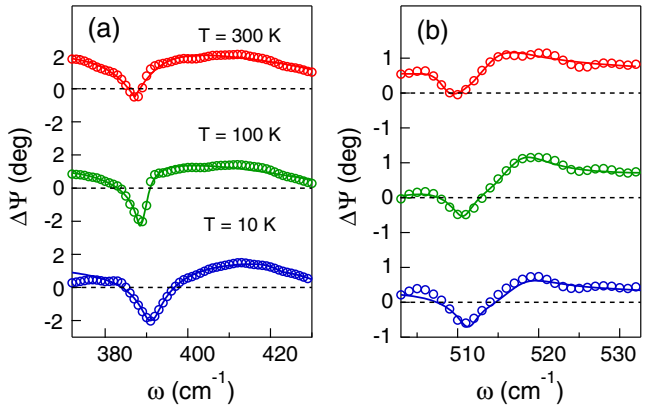

FIG. 3. Berreman resonances at the interface between Bi_2Se_3 and Al_2O_3, in the spectral regions of sapphire phonons (a) LO1 and (b) LO2, at three temperatures (circles). The solid lines are fitting curves obtained by the procedure described in the text.

TABLE I. Fitting parameters for the 2DES at the interface between Bi_2Se_3 and Al_2O_3, as obtained from the Berreman resonances at LO1 and LO2 shown in Fig. 3. The 2DES thickness d is in nm. All of the other values (2DES plasma frequencies ω_p and relaxation rates Γ_D, sapphire longitudinal phonon frequencies ω_{LO} and widths Γ_{LO}) are in cm^{-1}. The parameters indexed 1 (2) were extracted from the Berreman resonance at the sapphire longitudinal phonons LO1 (LO2). All phonon parameters of the sapphire substrate, as obtained from the fit to its reflectivity, are reported in Table I of the SM [27].

T (K)	d_1	ω_{p1}	Γ_{D1}	ω_{LO1}	Γ_{LO1}	d_2	ω_{p2}	Γ_{D2}	ω_{LO2}	Γ_{LO2}
300	0.7	8100	220	391	16	0.6	7700	190	482	39
100	0.8	8000	205	389	6	0.5	7950	175	484	22
10	0.5	8400	250	387	2	0.5	8050	200	485	16

1500 $cm^2/V\,s$ (depending on the film thickness) of Ref. [29]. Also the present determination of the 2DES thickness at the surface of a topological insulator—the first optical one to our knowledge—is close to the value reported in Ref. [8].

The results reported in Table I can greatly help one to identify the nature of the 2DES that we have observed here. As already mentioned, three species of free charges may contribute to the surface conductance: (a) TSS, (b) electrons from impurities and vacancies randomly distributed close to the surface, (c) electrons from impurities and vacancies which accumulate below the surface due to band folding effects. On the one hand, the spurious charges of (b) and (c) type are expected to be few for the following reasons: these MBE-grown Bi_2Se_3 films have been demonstrated in previous experiments [6,8] to be extremely pure, and the present value of $n_s = (8 \pm 2) \times 10^{12}$ cm^{-2} agrees with that extracted from those experiments (9×10^{12}). Moreover, n_s is constant between 10 and 300 K, while it should rapidly increase with T in a case of impurity ionization. On the other hand, two important findings are consistent with the attribution of the 2DES to TSSs. First, as already mentioned, its thickness $d \sim 1$ nm, smaller by 2 orders of magnitude than that of the Bi_2Se_3 film, is coherent with dc results [8]. Second, the relaxation rate Γ_D is constant with temperature, within errors, as already suggested by plasmonic experiments [11] and expected for the TSSs, which are extremely robust against nonmagnetic scattering processes.

In conclusion, we have used the Berreman effect to investigate, at wavelengths larger by 3 or 4 orders of magnitude than the thickness of the system to be investigated, the electrodynamics of the interface between a high-purity thin film of the topological insulator Bi_2Se_3 and its sapphire substrate. Indeed, the layer at the film-vacuum interface does not contribute to the present observations due to the nature of the BE and to its negligible direct absorption. Moreover, any interaction between the two opposite TSSs is excluded by the large Bi_2Se_3 film thickness. By accurate fits to the Berreman resonances at the reflectivity edges of two LO phonons of sapphire, we have determined for the 2DES a surface density and a mobility consistent with previous determinations on the same system by different techniques. The Fresnel formulas which fit to data the expression for the change in the ellipsometric angle $\Delta\Psi$ induced by the 2DES show that its thickness is smaller than 1 nm. Not only does this value obviously exclude that the observed conducting layer is the Bi_2Se_3 film itself, 120 nm thick, but it is also too small for a 2DES formed of charges accumulated by band bending below the interface. Estimates on the order of 1 nm have instead been proposed in the literature for the thickness of the TSS layer. Moreover, the extension of the present measurements to low temperature has shown that the Drude parameters of the 2DES are basically independent of T, demonstrating that (i) the charges are not thermally activated, as if they were produced from impurities or vacancies, and (ii) they are extremely robust against scattering processes. Thus, all of our findings consistently point toward the conclusion that the 2DES revealed by the Berreman effect is formed by topological surface states, whose infrared response has been detected here.

We are indebted to A. Millis and S. Park for the helpful discussions. This work has been partially supported by the Italian Ministry of University and Research through the PRIN project *OXIDE* and by the Sapienza University of Rome through funds Ateneo 2016 and Ateneo 2017. P. P. S., M. S., J. M., and S. O. are supported by the Gordon and Betty Moore Foundation's EPiQS Initiative (Grant No. GBMF4418) and the National Science Foundation (NSF) (Grant No. EFMA-1542798). We also acknowledge PALM LABEX funding (Project No. AIR2DES) for supporting P. C. during the development of the grazing incidence optical setup and SOLEIL for provision of beam time under Proposal No. 20170072. We also thank for their assistance all personnel of the AILES beam line.

[1] C. L. Kane and E. J. Mele, Phys. Rev. Lett. **95**, 226801 (2005).
[2] M. Z. Hasan and C. L. Kane, Rev. Mod. Phys. **82**, 3045 (2010).
[3] J. E. Moore, Nature (London) **464**, 194 (2010).
[4] H. Zhang, C.-X. Liu, X.-L. Qi, X. Dai, Z. Fang, and S.-C. Zhang, Nat. Phys. **5**, 438 (2009).
[5] N. P. Butch, K. Kirshenbaum, P. Syers, A. B. Sushkov, G. S. Jenkins, H. D. Drew, and J. Paglione, Phys. Rev. B **81**, 241301 (2010).
[6] M. Brahlek, N. Koirala, N. Bansal, and S. Oh, Solid State Commun. **215–216**, 54 (2015).
[7] Y. Zhang *et al.*, Nat. Phys. **6**, 584 (2010).
[8] N. Bansal, Y. S. Kim, M. Brahlek, E. Edrey, and S. Oh, Phys. Rev. Lett. **109**, 116804 (2012).

[9] M. Basletic, J.-L. Maurice, C. Carrero, G. Herranz, O. Copie, M. Bibes, E. Jacquet, K. Bouzehouane, S. Fusil, and A. Barthélémy, Nat. Mater. **7**, 621 (2008).
[10] A. Nucara, M. Corasaniti, A. Kalaboukhov, M. Ortolani, E. Falsetti, A. Sambri, F. Miletto Granozio, F. Capitani, J.-B. Brubach, P. Roy, U. Schade, and P. Calvani, Phys. Rev. B **97**, 155126 (2018).
[11] P. Di Pietro, M. Ortolani, O. Limaj, A. Di Gaspare, V. Giliberti, F. Giorgianni, M. Brahlek, N. Bansal, N. Koirala, S. Oh, P. Calvani, and S. Lupi, Nat. Nanotechnol. **8**, 556 (2013).
[12] T. P. Ginley and S. Law, Adv. Opt. Mater. **6**, 1800113 (2018).
[13] D. W. Berreman, Phys. Rev. **130**, 2193 (1963).
[14] A. Dubroka, M. Rössle, K. W. Kim, V. K. Malik, L. Schultz, S. Thiel, C. W. Schneider, J. Mannhart, G. Herranz, O. Copie, M. Bibes, A. Barthélémy, and C. Bernhard, Phys. Rev. Lett. **104**, 156807 (2010).
[15] M. Yazdi-Rizi, P. Marsik, B. P. P. Mallett, K. Sen, A. Cerreta, A. Dubroka, M. Scigaj, F. Sánchez, G. Herranz, and C. Bernhard, Phys. Rev. B **95**, 195107 (2017).
[16] P. Di Pietro, F. M. Vitucci, D. Nicoletti, L. Baldassarre, P. Calvani, R. Cava, Y. S. Hor, U. Schade, and S. Lupi, Phys. Rev. B **86**, 045439 (2012).
[17] B. Harbecke, B. Heinz, and P. Grosse, Appl. Phys. A **38**, 263 (1985).
[18] R. E. V. Profumo, R. Asgari, M. Polini, and A. H. MacDonald, Phys. Rev. B **85**, 085443 (2012).
[19] M. Dressel and G. Grüner, *Electrodynamics of Solids* (Cambridge University Press, Cambridge, England, 2002).
[20] N. Bansal, Y.-S. Kim, El. Edrey, M. Brahlek, Y.Horibe, K. Iida, M. Tanimura, G.-H. Li, T. Feng, H.-D. Lee, T. Gustafsson, E. Andrei, and S. Oh, Thin Solid Films **520**, 224 (2011).
[21] P. Roy, J.-B. Brubach, P. Calvani, G. De Marzi, A. Filabozzi, A. Gerschel, P. Giura, S. Lupi, O. Marcouillé, A. Mermet, A. Nucara, A. Paolone, and M. Vervloet, Nucl. Instrum. Methods Phys. Res., Sect. A **467–468**, 426 (2001).
[22] P. Roy, M. Rouzires, Z. Qi, and O. Chubar, Infrared Phys. Technol. **49**, 139 (2006).
[23] M. Schubert, T. E. Tiwald, and C. M. Herzinger, Phys. Rev. B **61**, 8187 (2000).
[24] G. Yu, N. L. Rowell, and D. J. Lockwood, J. Vac. Sci. Technol. A **22**, 1110 (2004).
[25] S. Y. Park and A. J. Millis, Phys. Rev. B **87**, 205145 (2013).
[26] F. Gervais, J.-L. Servoin, A. Baratoff, J. G. Bednorz, and G. Binnig, Phys. Rev. B **47**, 8187 (1993).
[27] See Supplemental Material at http://link.aps.org/supplemental/10.1103/PhysRevLett.121.176803 for details on data analysis, an explanation of the assumptions made, and phonon parameters of sapphire.
[28] L. Wu, W. K. Tse, M. Brahlek, C. M. Morris, R. V. Aguilar, N. Koirala, S. Oh, and N. P. Armitage, Phys. Rev. Lett. **115**, 217602 (2015).
[29] K. Dohunl, S. Cho, N. P. Butch, P. Syers, K. Kirshenbaum, S. Adam, J. Paglione, and M. S. Fuhrer, Nat. Phys. **8**, 459 (2012).